RESEARCH PAPER

Widespread structural brain involvement in ALS is not limited to the *C9orf72* repeat expansion

Henk-Jan Westeneng,[1] Renée Walhout,[1] Milou Straathof,[2] Ruben Schmidt,[1] Jeroen Hendrikse,[3] Jan H Veldink,[1] Martijn P van den Heuvel,[4] Leonard H van den Berg[1]

[1]Department of Neurology, Brain Center Rudolf Magnus, University Medical Center Utrecht, Utrecht, The Netherlands
[2]Biomedical MR Imaging and Spectroscopy Group, Center for Image Sciences, University Medical Center Utrecht, Utrecht, The Netherlands
[3]Department of Radiology, Brain Center Rudolf Magnus, University Medical Center Utrecht, Utrecht, The Netherlands
[4]Department of Psychiatry, Brain Center Rudolf Magnus, University Medical Center Utrecht, Utrecht, The Netherlands

Correspondence to
Professor Leonard H van den Berg, Department of Neurology, G03.228, University Medical Center Utrecht, P.O. Box 85500, Utrecht 3508 GA, The Netherlands; L.H.vandenberg@umcutrecht.nl

H-JW and RW contributed equally.

ABSTRACT

Background In patients with a *C9orf72* repeat expansion (C9+), a neuroimaging phenotype with widespread structural cerebral changes has been found. We aimed to investigate the specificity of this neuroimaging phenotype in patients with amyotrophic lateral sclerosis (ALS).

Methods 156 C9– and 14 C9+ patients with ALS underwent high-resolution T1-weighted MRI; a subset (n=126) underwent diffusion-weighted imaging. Cortical thickness, subcortical volumes and white matter integrity were compared between C9+ and C9– patients. Using elastic net logistic regression, a model defining the neuroimaging phenotype of C9+ was determined and applied to C9– patients with ALS.

Results C9+ patients showed cortical thinning outside the precentral gyrus, extending to the bilateral pars opercularis, fusiform, lingual, isthmus-cingulate and superior parietal cortex, and smaller volumes of the right hippocampus and bilateral thalamus, and reduced white matter integrity of the inferior and superior longitudinal fasciculus compared with C9– patients (p<0.05). Among 128 C9– patients, we detected a subgroup of 27 (21%) with a neuroimaging phenotype congruent to C9+ patients, while 101 (79%) C9– patients showed cortical thinning restricted to the primary motor cortex. C9– patients with a 'C9+' neuroimaging phenotype had lower performance on the frontal assessment battery, compared with other C9– patients with ALS (p=0.004).

Conclusions This study shows that widespread structural brain involvement is not limited to C9+ patients, but also presents in a subgroup of C9– patients with ALS and relates to cognitive deficits. Our neuroimaging findings reveal an intermediate phenotype that may provide insight into the complex relationship between genetic factors and clinical characteristics.

INTRODUCTION

Of the genes which have been associated with amyotrophic lateral sclerosis (ALS), a repeat expansion in the *C9orf72* gene is most commonly observed, contributing to 20–40% of the familial ALS cases and 5–10% of the patients with sporadic ALS in the Netherlands.[1] Previous research has demonstrated that patients with ALS with the *C9orf72* repeat expansion (C9+) show more cognitive and behavioural impairment compared with patients with ALS without the repeat expansion (C9–).[2]

MRI research has indicated that neurodegeneration in ALS is not restricted to the motor network; areas not directly involved in motor function also seem to be affected,[3] including frontotemporal areas[4–6] and subcortical structures.[7][8] More widespread involvement has been demonstrated in C9+ patients with ALS compared with C9– patients with ALS,[9] but whether this neuroimaging phenotype is specific for C9+ patients has not been investigated.

Considering the clinical heterogeneity of ALS, defining the patterns of neurodegeneration associated with C9– and C9+ ALS might shed light on the relation between structural brain involvement and clinical phenotypes, and might provide insight into the neurobiology of disease. Neuroimaging possibly reveals anatomical substrates of neuropsychological deficits as well as characteristic patterns of cerebral involvement in C9+ patients with ALS. It might contribute to our understanding about whether ALS is one disease or a collection of subtypes or a disease spectrum,[10] and might be useful for stratifying patients in future therapeutic trials.

In this study, we investigated the neuroimaging phenotype of C9+ patients with ALS using structural and diffusion-weighted MRI, and investigated whether this neuroimaging phenotype is specific for C9+ ALS.

METHODS

Participants

Patients were recruited from the outpatient clinic for motor neuron diseases at the University Medical Center Utrecht (UMC Utrecht). All patients were classified as having possible, probable or definite ALS according to the El Escorial Criteria. Clinical characteristics, including revised ALS Functional Rating Scale (ALSFRS-R), disease duration, age at onset, site of onset and handedness, were assessed. Fourteen C9+ and 156 C9– patients with ALS participated in this study. For comparison, 92 healthy controls were included as a reference group (see online supplementary table S1). Participants with a history of epilepsy, stroke or any overt structural brain abnormalities were excluded.

Standard protocol approvals, registrations and patient consents

This study was approved by the Medical Ethical Committee of the UMC Utrecht and written informed consent was obtained from all participants.

Cognitive assessment

The Verbal Fluency Index (VFI)[11][12] and Frontal Assessment Battery (FAB)[13] were used to assess cognitive performance in patients with ALS. The VFI

was calculated as previously described,[11] with higher VFI scores indicating more severe cognitive impairment. The FAB is a short cognitive and behavioural testing battery to assess executive function, with lower scores reflecting more severe frontal lobe dysfunction.[14]

Detection of C9orf72 repeat expansion

Genomic DNA samples of patients with ALS were screened for the *C9orf72* repeat expansion, using a repeat primed PCR as previously described.[1] Patients with a repeat length of at least 30 repeats were classified as C9+ patients with ALS.

MRI acquisition

Images were acquired using a 3 Tesla Achieva Medical Scanner from Philips. A high-resolution T1-weighted image was made using the following parameters: three-dimensional fast field echo using parallel imaging; repetition time/echo time (TR/TE) =10/4.6 ms, flip angel 8°, slice orientation sagittal, 0.75×0.75×0.8 mm voxel size, field of view=160× 240×240 mm and reconstruction matrix=200×320×320 covering the entire brain.

Diffusion-weighted imaging (DWI) was performed for reconstruction of major white matter tracts. Two sets of 30 weighted diffusion scans and 5 unweighted B0 scans were acquired with the following parameters: DWI using parallel imaging SENSE p-reduction 3; high angular gradient set of 30 different weighted directions, TR/TE=7035/68 ms, 2×2×2 mm voxel size, 75 slices, b=1000 s/mm^2, second set with reversed k-space read-out to correct for susceptibility-induced distortions.

Image preprocessing

T1-weighted images were preprocessed using Freesurfer V.5.3 (http://surfer.nmr.mgh.harvard.edu/). The cerebral cortex was parcellated into 68 regions[15] and segmented into 24 subcortical structures (deep grey matter, ventricles and cerebellum).[16]

DWI preprocessing included motion, eddy-current and susceptibility distortion corrections.[17] [18] Diffusion-weighted images were subsequently processed with the TRACULA tool (TRActs Constrained by UnderLying Anatomy) for automated reconstruction of major white matter tracts, using global probabilistic tractography.[19] Default settings for TRACULA were used including affine registration of diffusion-weighted images to T1-weighted images and estimation of probability distributions of diffusion measures in every voxel using a ball-and-stick model with two compartments (to account for possible crossing and kissing fibres). In total, 7500 Markov chain Monte-Carlo samples were obtained to estimate posterior distributions of the white matter tracts. The final output included anisotropy and diffusivity-weighted metrics of white matter tracts, including fractional anisotropy (FA) and radial diffusivity (RD).

Statistical analysis

Differences in clinical, cognitive and demographic data between research groups were assessed by χ^2 tests for categorical variables and linear models for continuous variables.

First, a region-wise analysis was performed analysing differences in cortical thickness per region. Second, a whole-brain vertex-wise comparison of cortical thickness was performed. Third, subcortical, cerebellar and ventricular volumes were measured with a region-wise analysis. FA and RD were compared between groups. Finally, we developed a model to capture the neuroimaging phenotype defining C9+ patients with ALS: the 'C9+' neuroimaging phenotype. On the basis of this model, patients with ALS were classified as having a 'C9+' neuroimaging phenotype or not.

Region-wise comparisons of C9+ and C9− patients with ALS were performed using linear modelling within the R software package for statistical computing V.3.1.0 (http://www.R-project. org). Age, gender and intracranial volume were used as covariates for all analyses, except for the analysis of white matter integrity, which included age and gender as covariates. To correct for possible non-normality, permutation tests (10 000 random permutations) were performed for all analyses. All analyses were corrected for multiple testing using false discovery rate (FDR). p Values <0.05, after correction for multiple testing, were considered to reflect statistically significant results. Original p values that reached statistical significance are reported.

In addition to the region-wise comparison of cortical thickness, a whole-brain vertex-wise comparison was performed using a linear model in Freesurfer. A cluster-wise correction was applied, using a Monte-Carlo simulation (10 000 iterations) with cluster threshold p<0.05. For comparison, the aforementioned analyses were repeated, comparing both C9+ and C9− patients with ALS to healthy controls (see online supplementary material).

To describe the pattern of brain involvement in C9+ ALS, we developed a model of structural imaging measures that distinguishes C9+ from C9− patients with ALS. To eliminate possible effects of age and gender on the classification as C9+ or C9−, we first fitted a linear model on all 92 brain regions of healthy participants (68 cortical regions and 24 subcortical regions) with age and gender as covariates. Subsequently, this model was used in a group of 170 patients with ALS (14 C9+ and 156 C9 + patients) to determine their dispersion (ie, residuals) from healthy controls per region. To find the variables defining the 'C9+' neuroimaging phenotype, elastic net (EN) logistic regression was performed. EN logistic regression is a form of penalised regression that provides simultaneous variable selection and shrinkage of the coefficients, thereby preventing overfitting (see online supplementary information 1 for information on EN logistic regression).[20] This analysis was performed in 14 C9+ patients with ALS and 28 C9− patients with ALS, who were age and gender matched to the 14 C9+ patients with ALS, selected out of the group of 156 C9− patients with ALS. To assess whether this model captures the characteristics of C9+ patients with ALS, classification accuracy of the model was determined in the data set with 14 C9− vs 28 C9+ patients with ALS. This was performed as a minimal assessment of the performance of the model. To investigate whether the 'C9+' neuroimaging phenotype was also present within the group of C9− patients with ALS, we subsequently applied the model to the remaining 128 C9− patients with ALS (who were not used to develop the model) to identify those with and without a 'C9+' neuroimaging phenotype. Model applications were performed by determining the linear predictor in the remaining 128 C9− patients with ALS, which was converted to a probability for belonging to the group with or without the 'C9+' imaging phenotype. The linear predictor was calculated by multiplication of the coefficients (as estimated using EN logistic regression during model development) with the values of the corresponding brain regions in the 128 C9− patients with ALS who were not used for model development (without adjustment or refitting of the model). Finally, we determined whether any clinical variables were related to the 'C9+' neuroimaging phenotype. For completeness, we repeated the analysis with additional inclusion of Diffusion tensor imaging (DTI) data (together with T1 data) in

the subgroup of patients with both DTI and T1 data (n=11). Results of this analysis should be interpreted with caution because of the smaller sample size while increasing the possible candidate predictors (ie, the FA and RD of the different tracts) which might cause instability of the model.

RESULTS

Clinical characteristics

Characteristics of the study participants are shown in table 1. C9+ patients with ALS were younger than C9− patients with ALS (p=0.049) and demonstrated a higher VFI than C9− patients with ALS (p=0.003; table 1). Frequency of bulbar onset of symptoms did not differ significantly between C9+ and C9− (p=0.53) and rate of decline was similar (p=0.72).

Cortical thickness: region-wise analysis

C9+ patients with ALS demonstrated more widespread cortical thinning compared with C9− patients with ALS, including cortical thinning in the bilateral superior parietal cortex (left: $p=4.91 \times 10^{-6}$; right: p=0.0006), cuneus (left: p=0.001; right: p=0.028), superior frontal cortex (left: p=0.0009; right: p=0.001) and lingual cortex (left: $p=3.59 \times 10^{-6}$; right: p=0.0006; figure 1A and see online supplementary table S2).

Compared with healthy controls, C9+ and C9− patients with ALS demonstrated different patterns of cerebral involvement as shown in online supplementary figure S1A and 1B. While C9− patients with ALS demonstrated cortical thinning restricted to the bilateral precentral gyrus (left: $p=5.6 \times 10^{-7}$; right: $p=4.51 \times 10^{-6}$), bilateral caudal middle frontal gyrus (left: p=0.005; right: p=0.004), right superior frontal (p=0.002) and right medial orbitofrontal gyrus (p=0.002), C9+ patients with ALS demonstrated cortical thinning in multiple brain regions including the bilateral pars opercularis (left: $p=6.08 \times 10^{-7}$; right: p=0.0002), inferior parietal cortex (left: $p=7.88 \times 10^{-6}$; right: p=0.002) and precuneus (left:

$p=1.99 \times 10^{-5}$; right: $p=2.37 \times 10^{-5}$; see online supplementary table S2). Similar outcomes were found with additional correction for bulbar onset.

Cortical thickness: whole-brain vertex-wise comparison

Vertex-wise comparison of C9+ and C9− patients with ALS showed significant cortical thinning in 10 clusters located in seven different areas (figure 1B). Bilateral cortical thinning was found in the superior parietal cortex (left: p=0.0001; right: p=0.0001), insula (left: p=0.0024; right: p=0.0366) and the isthmus of the cingulate cortex (left: p=0.032; right: p=0.0001). Moreover, clusters were found in the left lateral occipital cortex (p=0.0055), left pars opercularis (p=0.0076), left fusiform gyrus (p=0.0001) and right rostral middle frontal cortex (p=0.0001).

Subcortical and ventricular volumes, cerebellum

Involvement of the basal ganglia was observed in C9+ patients with ALS, showing significantly smaller volumes of the bilateral thalamus (left: p=0.001; right: p=0.0002), caudate nucleus (left: p=0.007; right: p=0.004), putamen (left: p=0.007; right: p=0.004), nucleus accumbens (left: p=0.010; right: p=0.001) and right hippocampus (p=0.008) compared with C9− patients with ALS (see online supplementary figure S2 and table S3). Moreover, the third (p=0.017) and fourth ventricles (p=0.003) were larger in C9+ patients with ALS as compared with C9− patients with ALS. Involvement of the cerebellum was observed by smaller volumes of the bilateral cerebellar cortex in C9+ patients with ALS (left: p=0.001; right: p=0.001).

Comparison of C9+ and C9− patients with ALS with healthy controls is shown in online supplementary table S3.

White matter integrity

DWI was available for a subset of participants (115 C9− patients with ALS, 11 C9+ patients with ALS and 75 healthy controls). Comparison of C9+ and C9− patients with ALS demonstrated significant differences in the bilateral inferior longitudinal fasciculus and in parietal and temporal parts of the superior longitudinal fasciculus. In the inferior longitudinal fasciculus, C9+ patients with ALS demonstrated a higher RD (left: p=0.002; right: p=0.0005) and lower FA bilaterally (left: p=0.002; right: p=0.002; figure 2 and online supplementary table S4). C9+ patients with ALS showed higher RD of the right temporal part (p=0.006) and parietal part (p=0.003) of the superior longitudinal fasciculus. C9+ patients with ALS showed a lower FA of the parietal part of the superior longitudinal fasciculus (p=0.003) compared with C9− patients with ALS.

Model development and application of the 'C9+' neuroimaging phenotype

EN logistic regression was performed in a group of 42 C9+ and C9− patients with ALS (ratio 1:2, ALS C9+ n=14 vs ALS C9− n=28; see flow chart in figure 3). Eleven out of 92 structural variables defined the 'C9+' neuroimaging phenotype (left hemisphere: cortical thickness of the fusiform gyrus, lingual gyrus, pars opercularis, isthmus of the cingulate and volume of the thalamus; right hemisphere: isthmus of the cingulate, thalamus, hippocampus, amygdala and nucleus accumbens; fourth ventricle (regression coefficients are shown in online supplementary figure S3)). These 11 imaging variables enabled accurate classification of 40 out of 42 patients into C9+ or C9− (95.2%). Next, we applied this model to the group of 128 C9− patients with ALS (156 minus 28 C9− patients with ALS of the training set) to

Table 1 Clinical and demographic characteristics of research groups

	C9+ ALS	C9− ALS
n	14	156
Male, n (%)	10 (71)	107 (69)
Age at MRI, median (range)	53.7 (40.6–67.0)	61.8 (24.0–78.9)
Right-handed, n (%)*	11 (92)	129 (91)
ALSFRS-R, median (range)	42 (33–47)	42 (23–48)
Age at onset, median (range)	52.9 (39.1–66.4)	60.9 (23.5–78.1)
Bulbar onset, n (%)	5 (36)	41 (26)
Disease duration in months, median (range)	12.3 (3.3–31.8)	12.0 (3.7–75.7)
Rate of decline, median (range)†	0.56 (0.15–1.14)	0.46 (0.00–3.92)
FAB score, median (range)‡	16 (13–18)	17 (6–18)
VFI score, median (range)§	12.9 (3.0–56.0)f	6.7 (3.2–24.9)f
ALS-FTD, n (%)¶	1 (7)	1 (1)
Familial ALS, n (%)	7 (50)f	10 (6)f
Survival in months, median (95% CI)	40.1 (28-NA)	35.6 (31.6 to 44.2)

*Handedness in a subset of patients; C9+ ALS: n=12, C9− ALS: n=141.
†Points decrease of ALSFRS-R per month.
‡FAB in a subset of patients (maximum score 18): C9+ ALS: n=9, C9− ALS: n=103.
§VFI in a subset of patients: C9+ ALS: n=8, C9− ALS: n=95.
¶ALS-FTD according to the Neary criteria.
fp<0.01.
ALSFRS-R, ALS-Functional Rating Scale Revised; ALS-FTD, amyotrophic lateral sclerosis with comorbid frontotemporal dementia; FAB, Frontal Assessment Battery; NA, not available; VFI, Verbal Fluency Index.
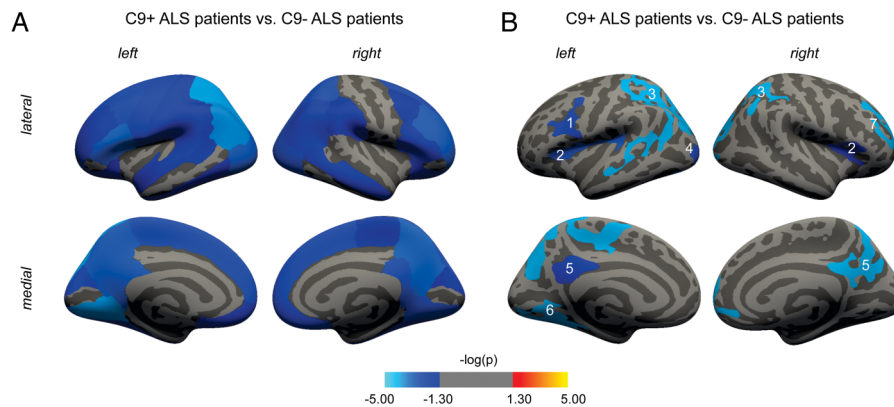
Figure 1 Region-wise and vertex-wise comparison of cortical thickness in C9− and C9+ patients with ALS. (A) Region-wise comparison of C9− and C9+ patients with ALS, showing widespread involvement of the cortex in C9+ patients with ALS. Blue-coloured areas show significant cortical thinning in C9+ patients with ALS compared with C9− patients with ALS (p<0.05, FDR-corrected). (B) Vertex-wise comparison between C9− and C9+ patients with ALS. Coloured clusters were significantly thinner in C9+ patients with ALS compared with C9− patients with ALS (cluster-wise corrected using a Monte-Carlo simulation with 10 000 iterations). 1=pars opercularis; 2=insula; 3=superior parietal (in the left hemisphere extending to the temporal lobe); 4=lateral occipital; 5=isthmus cingulate; 6=fusiform; 7=rostral middle frontal. ALS-FTD, amyotrophic lateral sclerosis with comorbid frontotemporal dementia; C9+, *C9orf72* repeat expansion present; C9−, *C9orf72* repeat expansion absent.
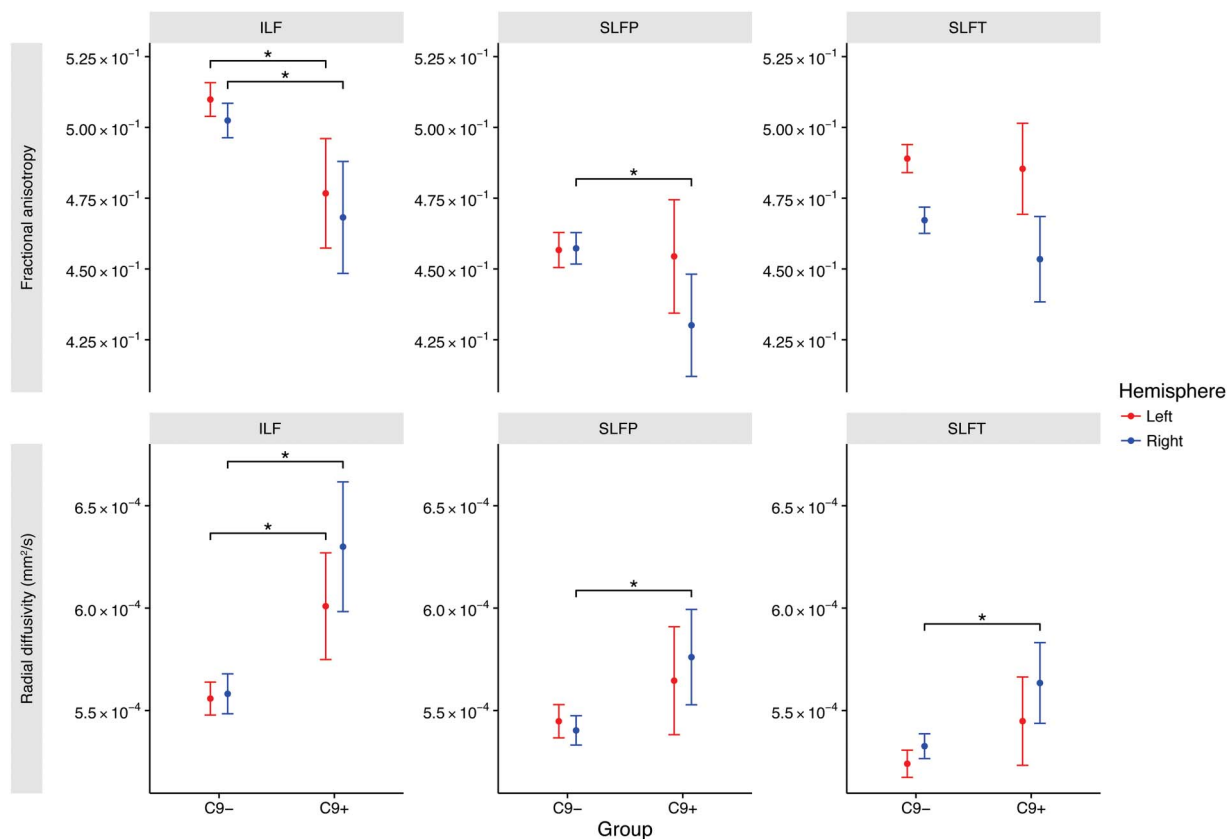

Figure 2 Comparison of white matter integrity in C9− and C9+ patients with ALS. The ILF is bilaterally affected in C9+ patients with ALS, characterised by an increased RD and lower FA, compared with C9− patients with ALS. SLFP and SLFT showed increased RD of the SLFP and SLFT in the right hemisphere of C9+ patients. Dots are estimated marginal means (ie, means corrected for effects of age and gender) and whiskers represent 95% CIs. Comparisons between groups and corresponding p values are shown in online supplementary table S4. *p value <0.05 after FDR correction. ALS-FTD, amyotrophic lateral sclerosis with comorbid frontotemporal dementia; FA, fractional anisotropy; ILF, inferior longitudinal fasciculus; RD, radial diffusivity; SLFP, parietal parts of the superior longitudinal fasciculus; SLFT, temporal parts of the superior longitudinal fasciculus.

potentially identify those with a 'C9+' neuroimaging phenotype (see online supplementary figure S4). This resulted in the classification of a subgroup of C9− patients with ALS with a 'C9+' neuroimaging phenotype characterised by extensive structural brain involvement (n=27, 21%), while the other C9− patients with

ALS (n=101, 79%) showed involvement restricted to the primary motor cortex on both sides (figure 4A). There was no difference between C9− patients with ALS and C9− patients with ALS with a 'C9+' neuroimaging phenotype regarding the 81 brain regions not included in the model (lowest p=0.304,
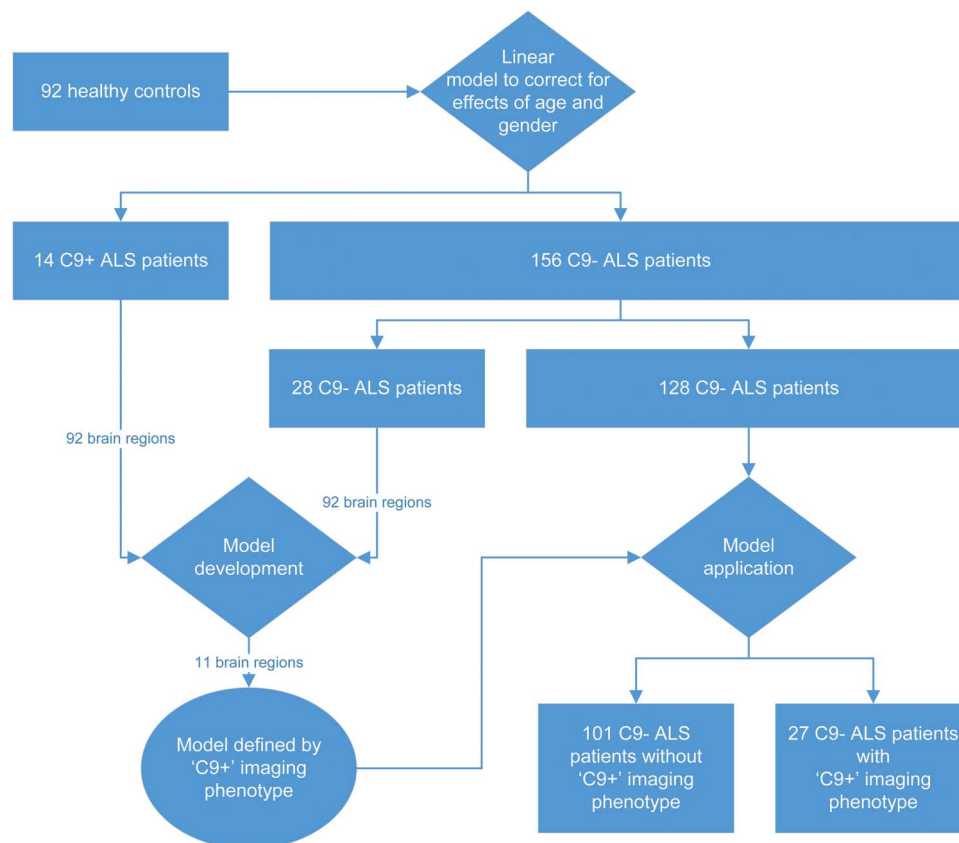
Figure 3 Flow chart of model development and application for classifying patients as C9+ or C9− based on neuroimaging phenotype. First, the model was developed in 14 C9+ patients with ALS and 28 age-matched and gender-matched C9− patients with ALS. A set of 11 imaging variables constituted the prediction model. Second, the model was applied to the remaining 128 C9− patients with ALS who were not used for model development. According to the model, 27 patients were classified with a 'C9+' neuroimaging phenotype and 101 patients with a C9− imaging phenotype. ACL, amyotrophic lateral sclerosis; C9+, *C9orf72* repeat expansion present; C9−, *C9orf72* repeat expansion absent.

FDR-corrected). Clinical characteristics of the groups are shown in figure 4B. C9− patients with ALS were younger than C9− patients with ALS with the 'C9+' neuroimaging phenotype (p=0.016); however, this difference in age could not be attributed to an implicit effect of age on the brain since classification was performed while effects of age and gender on the brain were eliminated. Regarding cognitive performance, C9− patients with ALS with a 'C9+' neuroimaging phenotype showed more executive dysfunction compared with C9− patients with ALS, as assessed by the FAB (p=0.004). There was no difference in survival between C9− patients with ALS and C9− patients with ALS with a 'C9+' neuroimaging phenotype (p=0.978). Repeating this analysis in the subgroup of patients with T1 and DTI data, we identified 24 C9− patients with a 'C9+' imaging phenotype out of 93 C9− patients (26%).

DISCUSSION
In this study, C9+ patients with ALS were found to have a neuroimaging phenotype with widespread cortical thinning, smaller volumes of deep grey matter structures and the cerebellar cortex, larger brain ventricles and involvement of frontal and temporal white matter tracts. We demonstrated that this neuroimaging phenotype is not limited to C9+ patients, but also present in a subgroup of C9− patients with ALS and relates to cognitive deficits. Apart from the *C9orf72* repeat expansion, other genetic or environmental factors might cause shared disease mechanisms underlying this neuroimaging phenotype.

Our results indicate that a comparable neuroimaging phenotype can be detected both in C9+ and a subgroup of C9− patients with ALS that extends to regions outside the primary motor area, including the basal ganglia and cerebellum. The basal ganglia are involved in motor and non-motor pathways.[21] Being part of frontal-subcortical circuits, involvement of these structures might contribute to the development of cognitive and behavioural changes in patients with ALS, as captured by a higher VFI of C9+ patients with ALS in this study. Decreased volume and changes in the shape of the thalamus in C9+ patients with ALS have been reported previously in imaging studies in ALS and frontotemporal dementia (FTD).[7 8 22] Involvement of the cerebellum in C9+ patients with ALS has been demonstrated by histological studies of *C9orf72* pathology.[23–26]

Besides extensive cortical and subcortical grey matter involvement, differences in white matter integrity between C9+ and C9− patients with ALS were also observed, including the inferior longitudinal fasciculus and superior longitudinal fasciculus. These white matter tracts constitute the connections between the frontal lobe and other lobes, and involvement of these tracts are potentially related to the higher incidence of cognitive and behavioural impairment in C9+ patients with ALS.[27]

By offering an intermediate phenotype, neuroimaging might provide the link between factors underlying the pathological mechanisms resulting in particular patterns of neurodegeneration and clinical phenotypes. Based on clinical and genetic research, cognitive and behavioural disturbances in ALS are now
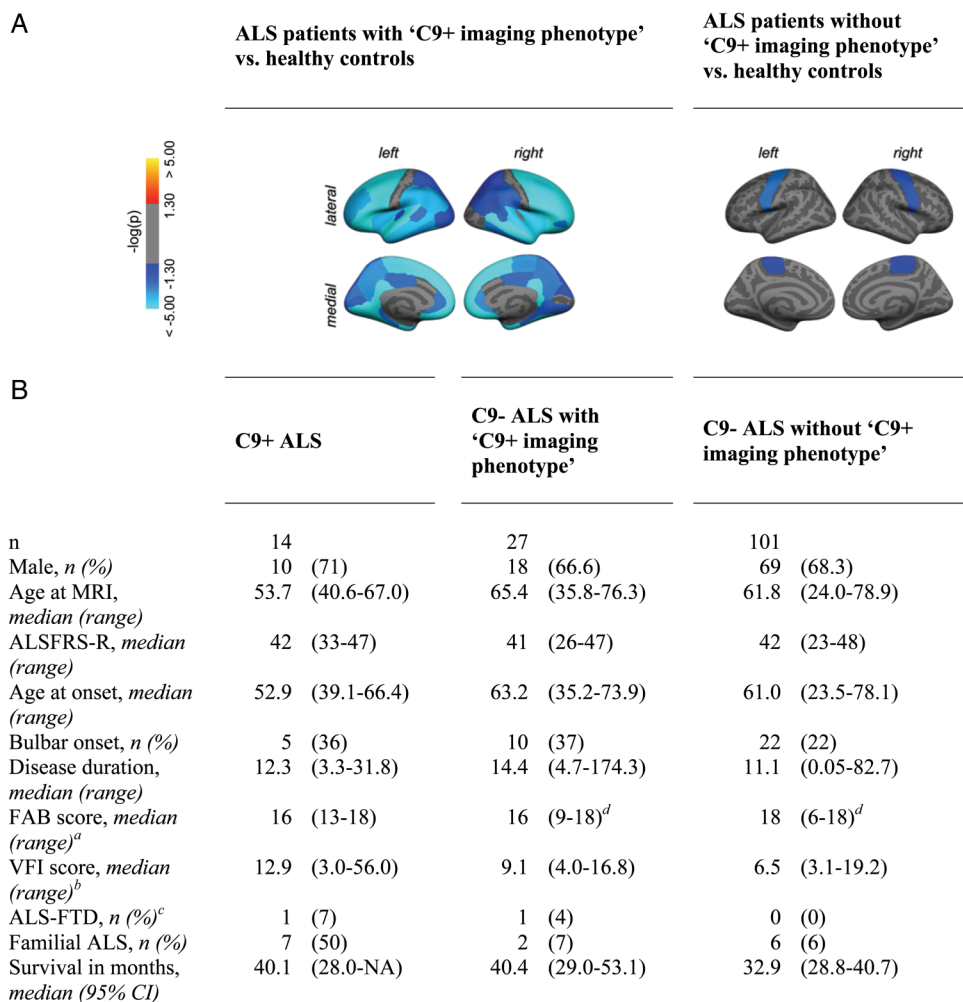
	C9+ ALS		C9− ALS with 'C9+ imaging phenotype'		C9− ALS without 'C9+ imaging phenotype'	
n	14		27		101	
Male, n (%)	10	(71)	18	(66.6)	69	(68.3)
Age at MRI, median (range)	53.7	(40.6-67.0)	65.4	(35.8-76.3)	61.8	(24.0-78.9)
ALSFRS-R, median (range)	42	(33-47)	41	(26-47)	42	(23-48)
Age at onset, median (range)	52.9	(39.1-66.4)	63.2	(35.2-73.9)	61.0	(23.5-78.1)
Bulbar onset, n (%)	5	(36)	10	(37)	22	(22)
Disease duration, median (range)	12.3	(3.3-31.8)	14.4	(4.7-174.3)	11.1	(0.05-82.7)
FAB score, median (range)[a]	16	(13-18)	16	(9-18)[d]	18	(6-18)[d]
VFI score, median (range)[b]	12.9	(3.0-56.0)	9.1	(4.0-16.8)	6.5	(3.1-19.2)
ALS-FTD, n (%)[c]	1	(7)	1	(4)	0	(0)
Familial ALS, n (%)	7	(50)	2	(7)	6	(6)
Survival in months, median (95% CI)	40.1	(28.0-NA)	40.4	(29.0-53.1)	32.9	(28.8-40.7)

Figure 4 Identification of patients with a *C9orf72* neuroimaging phenotype in a group of C9− patients with ALS. (A) Elastic net logistic regression identified a characteristic pattern of brain involvement distinguishing C9+ from C9− patients with ALS based on 11 imaging variables, the 'C9+' neuroimaging phenotype. Patients with ALS were subsequently classified into patients with and without this characteristic neuroimaging phenotype, and cortical thickness was compared in a region-wise analysis with healthy controls (n=92). Blue-coloured areas show significant cortical thinning in patients with ALS compared with healthy controls (p<0.05, FDR-corrected). (B) Classification of a subgroup of 128 C9− patients with ALS (156 minus 28 C9− patients with ALS of the training set) revealed 27 C9− patients with ALS with a 'C9+' neuroimaging phenotype with widespread cortical involvement congruent to C9+ patients with ALS (n=14), whereas 101 C9− patients with ALS had a phenotype of cortical thinning restricted to the primary motor areas. Clinical characteristics are shown per study group. [a]FAB in a subset of patients (maximum score 18): C9+ ALS n=9, C9− ALS with 'C9+' neuroimaging phenotype n=18, C9− ALS without 'C9+' neuroimaging phenotype n=67. [b]VFI in a subset of patients: C9+ ALS n=8, C9− ALS with 'C9+' neuroimaging phenotype n=14, C9− ALS without 'C9+' neuroimaging phenotype n=64. [c]ALS-FTD according to the Neary criteria. [d]p<0.01 (Mann-Whitney U). ALS-FRS R, ALS-Functional Rating Scale Revised; ALS-FTD, amyotrophic lateral sclerosis with comorbid frontal temporal dementia; FAB, Frontal Assessment Battery; NA, not available; VFI, Verbal Fluency Index.

recognised as an important part of the ALS-FTD disease spectrum.[28] The results of our study shed light on the complex relationship between genetics, cerebral changes and cognition by showing that the neuroimaging phenotype with widespread structural involvement found in C9+ patients with ALS may also be present in C9− patients with ALS. Involvement of regions outside the primary motor areas might relate to cognitive deficits found in patients with ALS. Cognitive assessment in this study was limited to the VFI in 60% and FAB in 66% of the patients with ALS. However, C9+ patients with ALS had a lower performance on the VFI, and C9− patients with ALS with a 'C9+' neuroimaging phenotype performed worse on the FAB. Since most of the patients were included and scanned before a Dutch version of the Edinburgh Cognitive and Behavioural ALS Screen (ECAS) had been validated,[29] ECAS data were not available, leaving the precise clinical manifestation in terms of

cognitive and behavioural deficits to be further explored. Cognitive and behavioural impairment might have compromised study participation in our study,[30] thereby introducing a selection bias towards less severely affected C9+ and C9− patients with ALS. Selection bias might also explain a relatively longer survival in C9+ patients in this study compared with a previously published paper from our group involving a population-based cohort.[1] More extensive cognitive and behavioural testing will further elucidate the profile of cognitive and behavioural deficits resulting from the pattern of cerebral involvement that is encountered in the 'C9+' neuroimaging phenotype.

Involvement of regions that in this study were found to differ between C9+ and C9− patients was, apart from the left isthmus, not reported in a previous study in asymptomatic carriers of a *C9orf72* repeat expansion,[31] suggesting that structural changes in most regions are specifically related to the

symptomatic stage of disease. We showed that neuroimaging phenotypes of patients with known mutations might be used as prior information to discover subgroups of patients with sporadic ALS who could not be detected by comparisons of groups of patients with ALS with healthy participants (see online supplementary figure S1A). Furthermore, our study demonstrates that neuroimaging in ALS may offer a detailed intermediate phenotype, providing a link between genetics and clinical presentation and suggests that other currently unknown factors might result in shared disease mechanisms and clinical phenotypes. This approach might lead to increased power to discover new genetic or environmental factors involved in ALS.

REFERENCES

1. van Rheenen W, van Blitterswijk M, Huisman MH, *et al*. Hexanucleotide repeat expansions in C9ORF72 in the spectrum of motor neuron diseases. *Neurology* 2012;79:878–82.
2. Byrne S, Elamin M, Bede P, *et al*. Cognitive and clinical characteristics of patients with amyotrophic lateral sclerosis carrying a C9orf72 repeat expansion: a population-based cohort study. *Lancet Neurol* 2012;11:232–40.
3. Foerster BR, Welsh RC, Feldman EL. 25 years of neuroimaging in amyotrophic lateral sclerosis. *Nat Rev Neurol* 2013;9:513–24.
4. Strong MJ. The syndromes of frontotemporal dysfunction in amyotrophic lateral sclerosis. *Amyotroph Lateral Scler* 2008;9:323–38.
5. Verstraete E, Veldink JH, Hendrikse J, *et al*. Structural MRI reveals cortical thinning in amyotrophic lateral sclerosis. *J Neurol Neurosurg Psychiatr* 2012;83:383–8.
6. Rajagopalan V, Pioro EP. Distinct patterns of cortical atrophy in ALS patients with or without dementia: an MRI VBM study. *Amyotroph Lateral Scler Frontotemporal Degener* 2014;15:216–25.
7. Bede P, Elamin M, Byrne S, *et al*. Basal ganglia involvement in amyotrophic lateral sclerosis. *Neurology* 2013;81:2107–15.
8. Westeneng HJ, Verstraete E, Walhout R, *et al*. Subcortical structures in amyotrophic lateral sclerosis. *Neurobiol Aging* 2015;36:1075–82.
9. Bede P, Bokde AL, Byrne S, *et al*. Multiparametric MRI study of ALS stratified for the C9orf72 genotype. *Neurology* 2013;81:361–9.
10. Andersen PM. Mutation in C9orf72 changes the boundaries of ALS and FTD. *Lancet Neurol* 2012;11:205–7.
11. Abrahams S, Leigh PN, Harvey A, *et al*. Verbal fluency and executive dysfunction in amyotrophic lateral sclerosis (ALS). *Neuropsychologia* 2000;38:734–47.
12. Thurstone LL, Thurstone TG. *Primary mental abilities*. Chicago: Science Research Associates, 1962.
13. Dubois B, Slachevsky A, Litvan I, *et al*. The FAB: a frontal assessment battery at bedside. *Neurology* 2000;55:1621–6.
14. Goldstein LH, Abrahams S. Changes in cognition and behaviour in amyotrophic lateral sclerosis: nature of impairment and implications for assessment. *Lancet Neurol* 2013;12:368–80.
15. Fischl B, van der Kouwe A, Destrieux C, *et al*. Automatically parcellating the human cerebral cortex. *Cereb Cortex* 2004;14:11–22.
16. Fischl B, Salat DH, van der Kouwe AJ, *et al*. Sequence-independent segmentation of magnetic resonance images. *Neuroimage* 2004;23(Suppl 1):S69–84.
17. Andersson JL, Skare S, Ashburner J. How to correct susceptibility distortions in spin-echo echo-planar images: application to diffusion tensor imaging. *Neuroimage* 2003;20:870–88.
18. Andersson JL, Sotiropoulos SN. Non-parametric representation and prediction of single- and multi-shell diffusion-weighted MRI data using Gaussian processes. *Neuroimage* 2015;122:166–76.
19. Yendiki A, Panneck P, Srinivasan P, *et al*. Automated probabilistic reconstruction of white-matter pathways in health and disease using an atlas of the underlying anatomy. *Front Neuroinform* 2011;5:23.
20. Zou H, Hastie T. Regularization and variable selection via the elastic net. *J R Stat Soc B* 2005;67:301–20.
21. Sharma KR, Saigal G, Maudsley AA, *et al*. 1H MRS of basal ganglia and thalamus in amyotrophic lateral sclerosis. *NMR Biomed* 2011;24:1270–6.
22. Mahoney CJ, Beck J, Rohrer JD, *et al*. Frontotemporal dementia with the C9ORF72 hexanucleotide repeat expansion: Clinical, neuroanatomical and neuropathological features. *Brain* 2012;135:736–50.
23. Al-Sarraj S, King A, Troakes C, *et al*. p62 positive, TDP-43 negative, neuronal cytoplasmic and intranuclear inclusions in the cerebellum and hippocampus define the pathology of C9orf72-linked FTLD and MND/ALS. *Acta Neuropathol* 2011;122:691–702.
24. Troakes C, Maekawa S, Wijesekera L, *et al*. An MND/ALS phenotype associated with C9orf72 repeat expansion: Abundant p62-positive, TDP-43-negative inclusions in cerebral cortex, hippocampus and cerebellum but without associated cognitive decline. *Neuropathology* 2012;32:505–14.
25. Prell T, Grosskreutz J. The involvement of the cerebellum in amyotrophic lateral sclerosis. *Amyotroph Lateral Scler Frontotemporal Degener* 2013;14:507–15.
26. Tan RH, Devenney E, Dobson-Stone C, *et al*. Cerebellar integrity in the amyotrophic lateral sclerosis-frontotemporal dementia continuum. *PLoS ONE* 2014;9:e105632.
27. Irwin DJ, McMillan CT, Brettschneider J, *et al*. Cognitive decline and reduced survival in C9orf72 expansion frontotemporal degeneration and amyotrophic lateral sclerosis. *J Neurol Neurosurg Psychiatry* 2013;84:163–9.
28. Phukan J, Pender NP, Hardiman O. Cognitive impairment in amyotrophic lateral sclerosis. *Lancet Neurol* 2007;6:994–1003.
29. Abrahams S, Newton J, Niven E, *et al*. Screening for cognition and behaviour changes in ALS. *Amyotroph Lateral Scler Frontotemporal Degener* 2014;15:9–14.
30. Alzheimer's Association. Research consent for cognitively impaired adults: recommendations for institutional review boards and investigators. *Alzheimer Dis Assoc Disord* 2004;18:171–5.
31. Walhout R, Schmidt R, Westeneng HJ, *et al*. Brain morphologic changes in asymptomatic C9orf72 repeat expansion carriers. *Neurology* 2015;85:1780–8.